UMBC
AN HONORS UNIVERSITY IN MARYLAND

Radio Frequency Interference Detection for Passive Remote Sensing Using Eigenvalue Analysis

Adam Schoenwald
(University of Maryland, Baltimore County)
(NASA Goddard Space Flight Center)

Dr. Seung-Jun Kim (University of Maryland, Baltimore County)
Dr. Priscilla Mohammed, (Morgan State University)

Acronym List

Acronym	Definition
ABS()	Absolute Value
AS&D	ASRC Federal Space and Defense
AUC	Area Under Curve
CERBM	Complex Entropy Rate Bound Minimization
CONUS	Continental United States
CQAMSYM	Complex Quadrature Amplitude Modulation
CSK	Complex Signal Kurtosis
CW	Continuous Wave
dB	Decibel
DDC	Digital Down Converter
DSP	Digital Signal Processing
DVB-S2	Digital Video Broadcasting - Satellite - Second Generation
ERBM	Entropy Rate Bound Minimization
ESTO	Earth Science Technology Office
FB	Full Band
FPGA	Field Programmable Gate Array
Gbps	Billions of Bits per Second
GMI	GPM Microwave Imager
GPM	Global Precipitation Measurement
GSFC	Goddard Space Flight Center

Acronym	Definition
H	Horrizontal
ICA	Independent Component Analysis
INR	Interference to Noise Ratio
MME	Maximum Minimum Eigenvalue ratio
MSE	Mean Square Error
NASA	National Aeronautics and Space Administration
NCCFASTICA	Non Circular Complex Fast ICA
PI	Principal Investigator
QPSK	Quadrature Phase Shift Keying)
RADAR	RAdio Detection And Ranging
RF	Radio Frequency
RFI	Radio Frequency Interference
ROACH	Reconfigurable Open Architecture Computing Hardware
ROC	Receiver Operating Characteristic
RRCOS	Root Raise Cosine
RSK	Real Signal Kurtosis
SB	Sub Band
SERDES	Serializer / Deserializer
SMAP	Soil Moisture Active Passive
V	Vertical

Motivation

- Unmitigated RFI (Radio Frequency Interference) can cause errors in science measurements
  - L- and C-Band: soil moisture measurements over land
  - L-, C- and X-band: ocean salinity, sea surface temperature, wind speed direction
  - K band: water vapor, liquid water
- Approach
  - RF front end development for 18 GHz (K band)
    - These allocations are known to be corrupted by direct broadcast services
  - Digital back end to allow sophisticated RFI detection and mitigation techniques

L, X band RFI

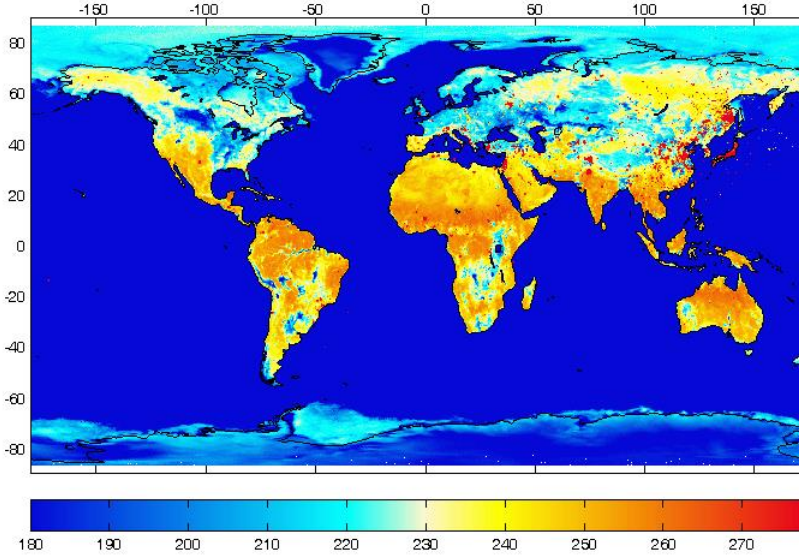

SMAP TA H-pol
1400 MHz

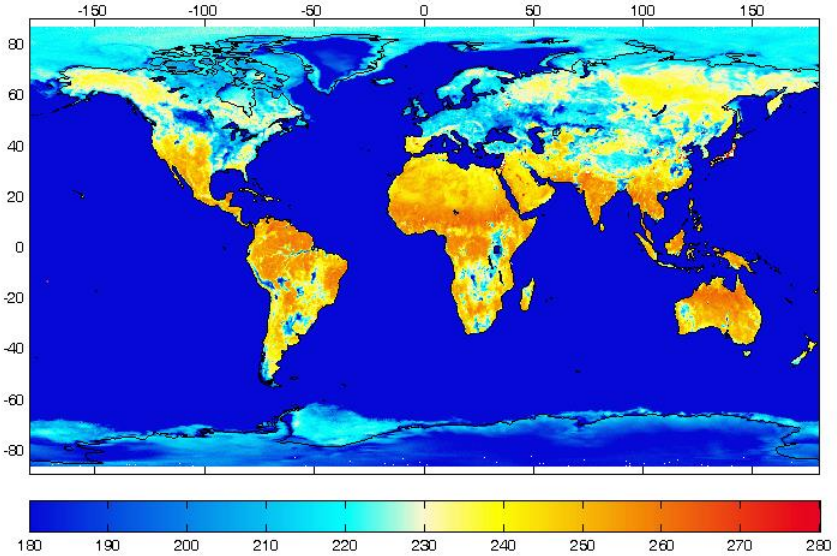

SMAP TA H-pol filtered

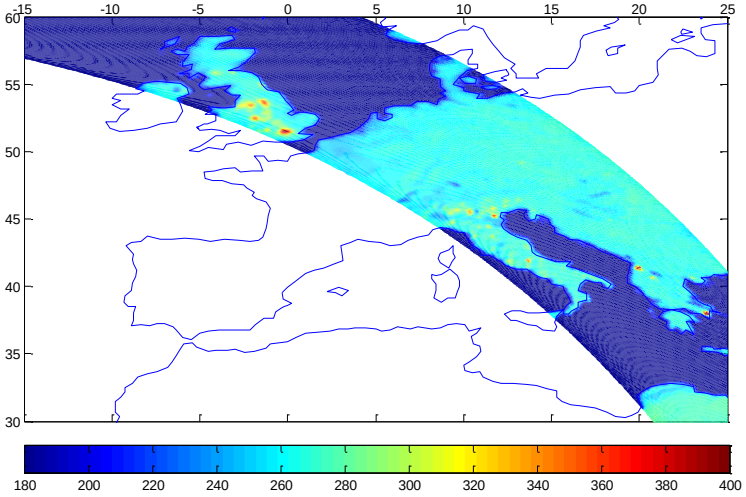

10 GHz GMI
Tb V-pol
(Vertical)

SMAP (Soil Moisture Active Passive) algorithms developed previously under ESTO (Earth Science Technology Office)

RFI from Geosynchronous Satellites Reflecting from the Surface

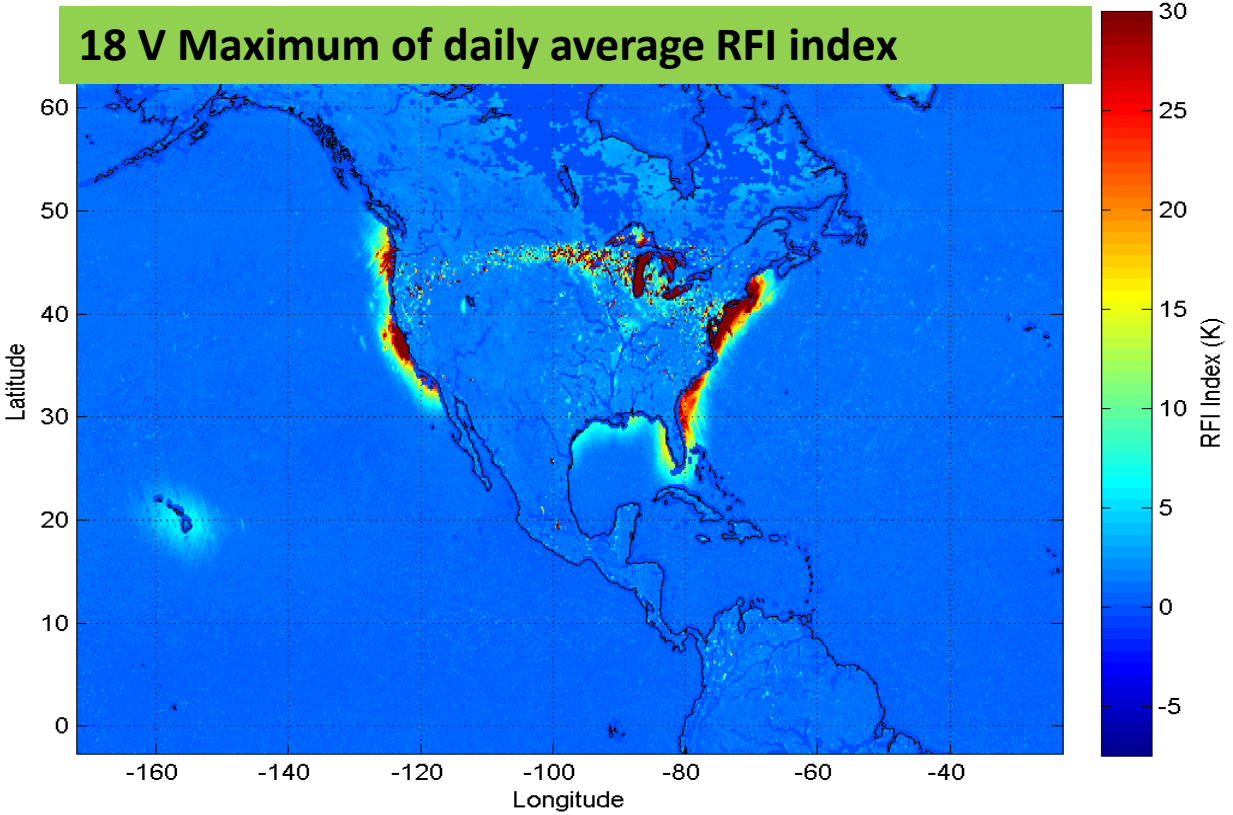

GMI data

Picture from David W. Draper, [1]

The 18 GHz Channel sees significant RFI from surface reflections around CONUS (Continental United States) and Hawaii

Real Signal Kurtosis (RSK)

Given a complex baseband signal $z(n) = I(n) + jQ(n)$, the fourth standardized moment is computed independently for both the real and imaginary vectors, I and Q, as was used in SMAP[3].

$$\mathrm{RSK_I} = \frac{\mathbb{E}[(\mathrm{I}-\mathbb{E}[\mathrm{I}])^4]}{(\mathbb{E}[(\mathrm{I}-\mathbb{E}[\mathrm{I}])])^2} - 3 \quad , \quad \mathrm{RSK_Q} = \frac{\mathbb{E}[(\mathrm{Q}-\mathbb{E}[\mathrm{Q}])^4]}{(\mathbb{E}[(\mathrm{Q}-\mathbb{E}[\mathrm{Q}])])^2} - 3$$

The test statistic, RSK [2,3] (Real Signal Kurtosis), is then defined as

$$\mathrm{RSK} = \frac{|\mathrm{RSK_I}| + |RSK_Q|}{2}$$

Complex Signal Kurtosis

Complex signal kurtosis (CSK) [4,5] is used to improve ability of the digital radiometer to detect RFI. It makes use of additional information in complex signals.

Given a complex baseband signal $z(n) = I(n) + jQ(n)$, *moments* $\alpha_{\ell,m}$ of $z(n)$ are defined as

$$\alpha_{\ell,m} = \mathbb{E}\left[(z - \mathbb{E}[z])^{\ell}(z - \mathbb{E}[z])^{*m}\right], \ell, m \in \mathbb{R} \geq 0$$

With $\sigma^2 = \alpha_{1,1}$, *Standardized moments* $\varrho_{\ell,m}$ can then be found as

$$\varrho_{\ell,m} = \frac{\alpha_{\ell,m}}{\sigma^{\ell+m}}$$

Leading to the CSK (Complex Signal Kurtosis) RFI test statistic used [4].

$$C_K = \frac{\varrho_{2;2} - 2 - \left|\varrho_{2;0}\right|^2}{1 + \frac{1}{2}\left|\varrho_{2;0}\right|^2}$$

Independent Component Analysis

- ICA [6] uses higher order statistics to perform blind source separation
- This suggests it may be useful for separating RFI from Gaussian noise in the radiometry context, studied in [7].
- We assume noise and RFI are statistically independent sources, mixing is linear, sources are non Gaussian
- Mixture model: **x = As**, observe **x**
- $\hat{\boldsymbol{s}}$ **= Wx**, $\hat{\boldsymbol{s}}$ is the estimated independent source

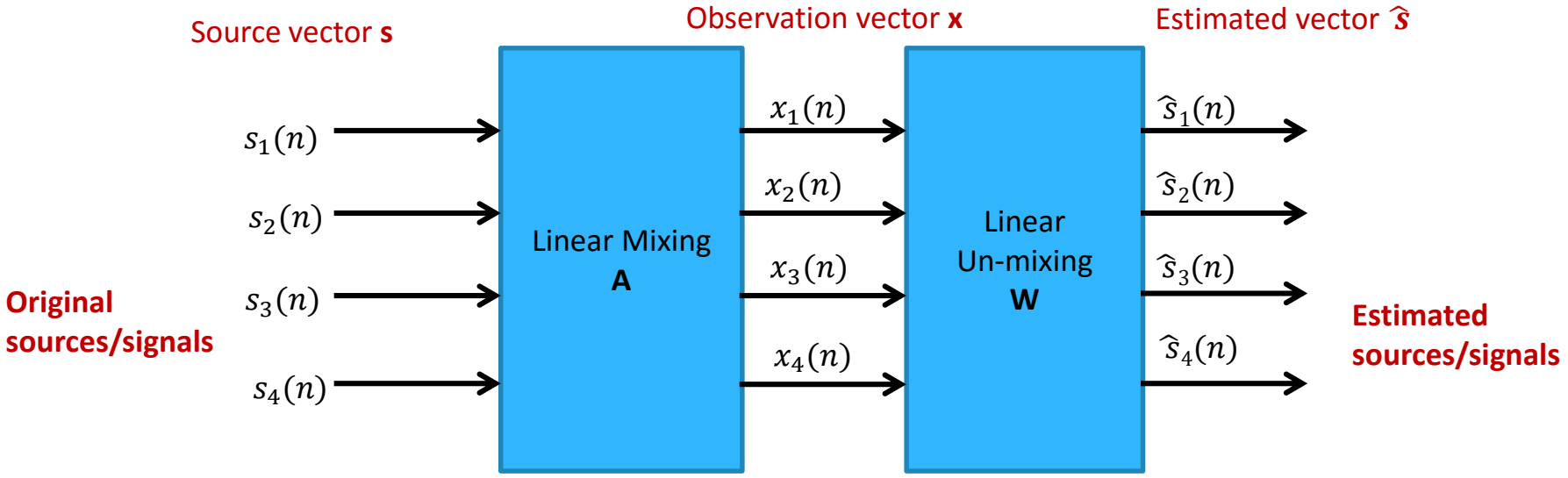

ICA RFI Detection

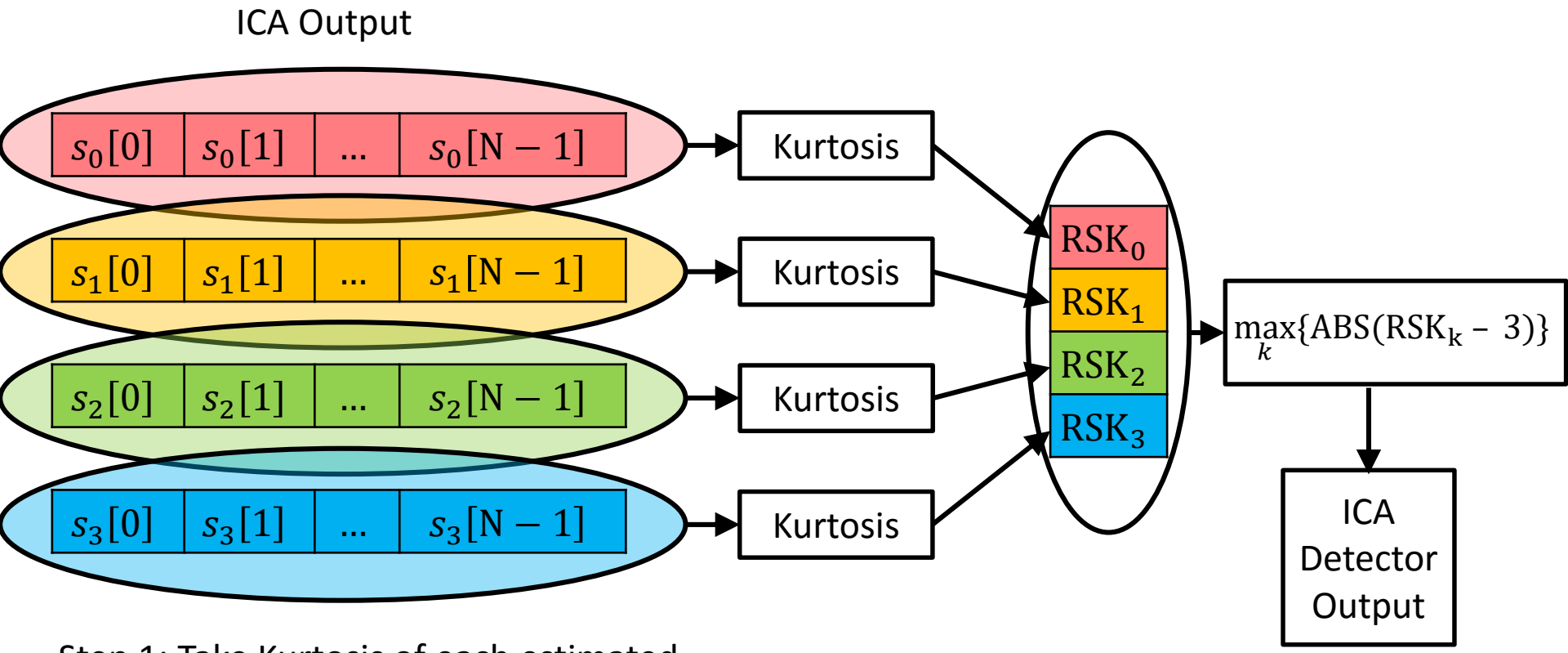

Step 1: Take Kurtosis of each estimated independent component vector

Step 2: Select the kurtosis value that deviated the furthest from 3

ROC Curves and AUC

- Each point on an ROC curve can be represented by the set {FAR, PD}
  - {False alarm Rate , Probability of Detection}
- ROC curves will generate from (0,0) to (1,1) by varying the threshold
- Poor detectors are close to the 1:1 line
- Better detectors show higher PD and smaller FAR
- **Figure of Merit = Area Under Curve (AUC)**
  - 0.5≤AUC ≤1
  - When AUC = 0.5 detector does not work
  - When AUC = 1 the detector works perfectly

Better Detection

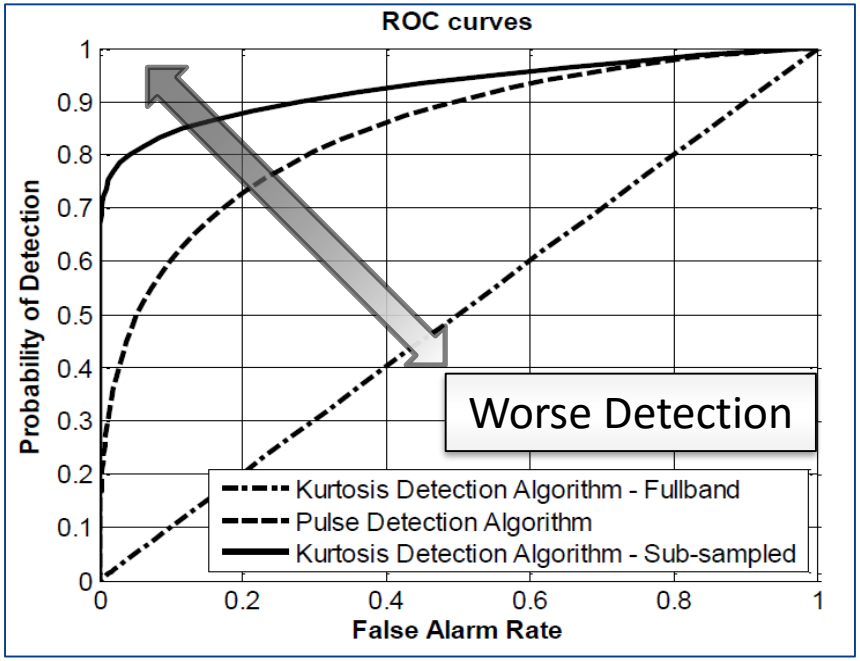

ROC curve example, from [8].

AUC = 1 ⟷ AUC = 0.5

Better Detection

Worse Detection

AUC Results- ICA Performance - CW

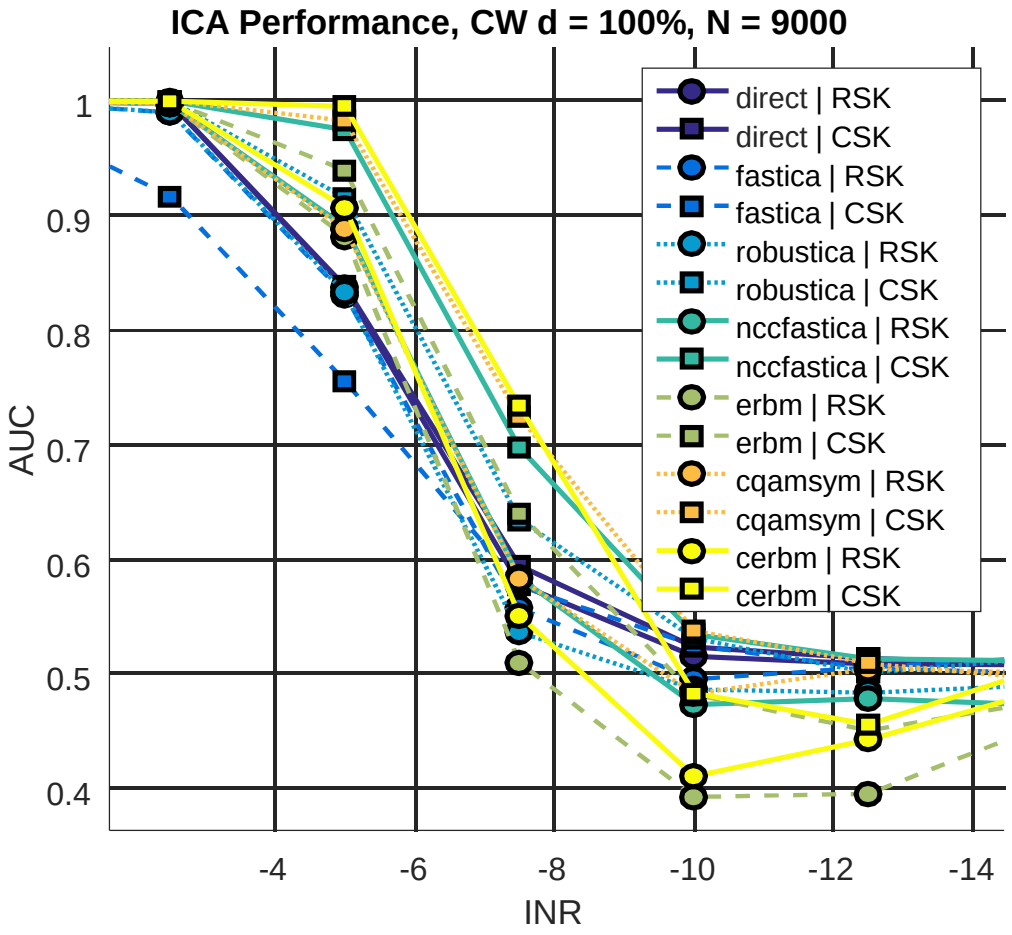

More ICA results in [7], generally a marginal improvement in detection is seen

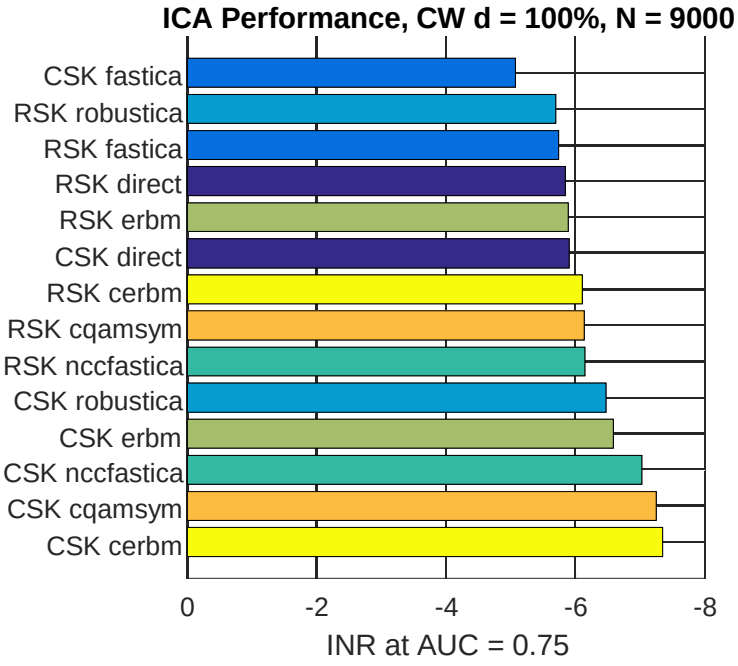

Various ICA algorithms are tested [9,10,11,12,13,14,15,16,17].
No ICA pre-processing is done on 'direct' data sets.

RSK = Real Signal Kurtosis
CSK = Complex Signal Kurtosis

Eigenvalue Approach

- Two objectives:
  - Detection: Identify power measurements that have been contaminated with interference
    - The Minimum Maximum Eigenvalue (MME) approach, adapted from the cognitive radio context [10], is applied here for RFI detection in passive remote sensing.
  - Excision: Accurately guess what the power measurement would have been if the interfere were not there

Conceptual Signal Model

Hypothesis Test / Signal Model

$$\mathcal{H}_0: x[k] = w[k]$$
$$\mathcal{H}_1: x[n] = w[k] + r[k]$$

$$SNR = \frac{P_s}{\sigma_w^2} \qquad \mathrm{P_s} = \mathrm{E}[(r[k])^2]$$

$w[k] \sim \mathcal{N}(0, \sigma_w^2)$ = Thermal Noise
$r[k]$ = RFI

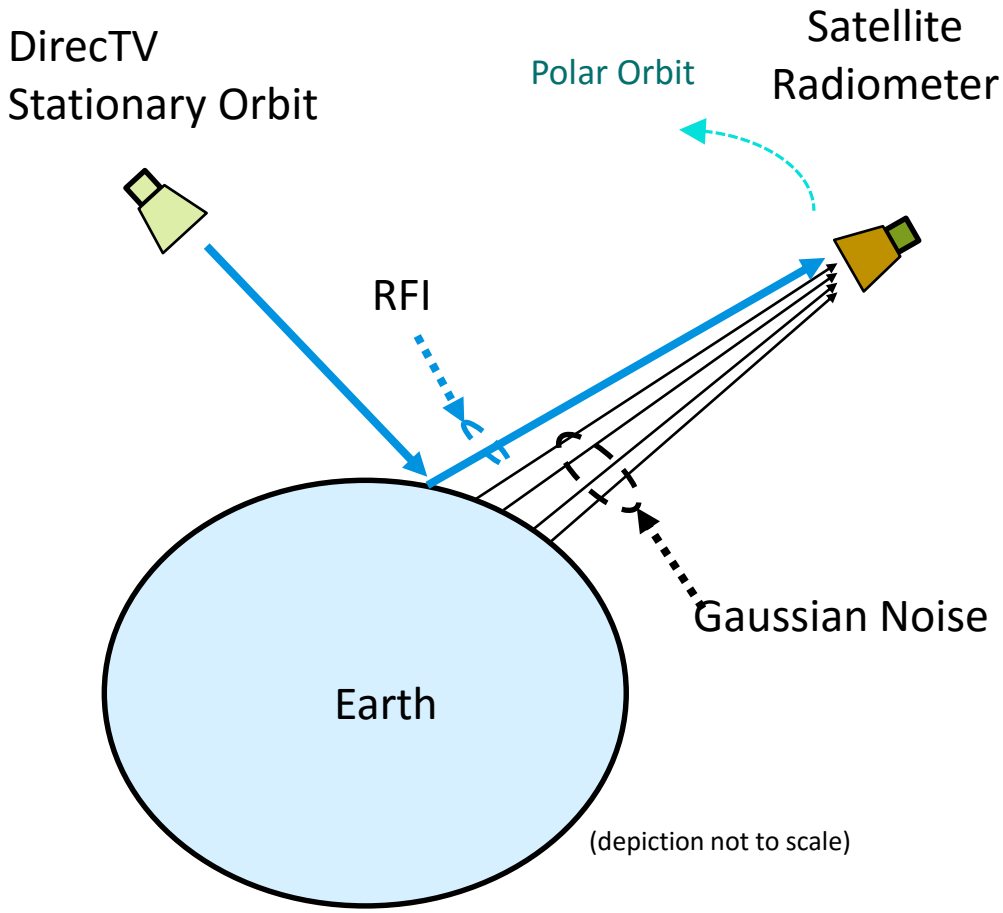

Measure the Sample Covariance (Oversampled)

Given our sampled signal x,

$$x_i(n) \equiv x[nM + i - 1] \quad i = 1,2, \dots, M$$

$$\mathbf{x}(n) \equiv [x_1(n), x_2(n), \dots x_M(n)]^T$$

$$\hat{\mathbf{x}}(n) \equiv [\mathbf{x}^T(n), \mathbf{x}^T(n-1), \dots \mathbf{x}^T(n-L+1)]^T$$

$$\mathbf{R}_x = \mathbb{E}[\hat{\mathbf{x}}(n)\hat{\mathbf{x}}^H(n)]$$

$$\mathbf{R}_x(N_s) \equiv \frac{1}{N_s} \sum_{n=L-1}^{L-2+N_s} \hat{\mathbf{x}}(n)\hat{\mathbf{x}}^H(n)$$

The Eigenvalues of the covariance matrix are found

$$\lambda_1 > \lambda_2 > \cdots > \lambda_{ML}$$

The test statistic is then formed as

$$\mathbf{T}_\lambda = \frac{\lambda_{max}}{\lambda_{min}}$$

Eigenvalue Noise Power Estimate

Scale the minimum eigenvalue of the covariance matrix to estimate the variance of the Gaussian thermal noise. The limiting distributions from [19] help derive the scaling factor.

$$\mathbf{R}_x \rightarrow \lambda_1 > \lambda_2 > \ \ldots \geq \lambda_{ML}$$

$$\lim_{N_s \rightarrow \infty} \lambda_{min} = \sigma^2 (1 \ - \sqrt{y})^2$$

$$\lim_{N_s \rightarrow \infty} \lambda_{max} = \sigma^2 (1 + \sqrt{y})^2$$

$$\widehat{\sigma_{\mathrm{w}}^2} = \lambda_{min} \frac{N_s}{\left(\sqrt{N_s} - \sqrt{ML}\right)}$$

Wideband RFI – 5 QPSK Channels

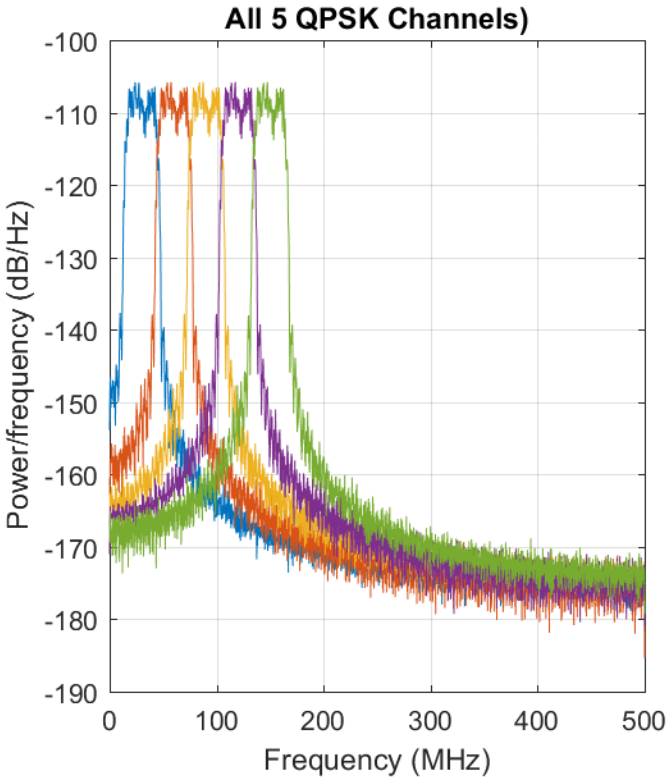

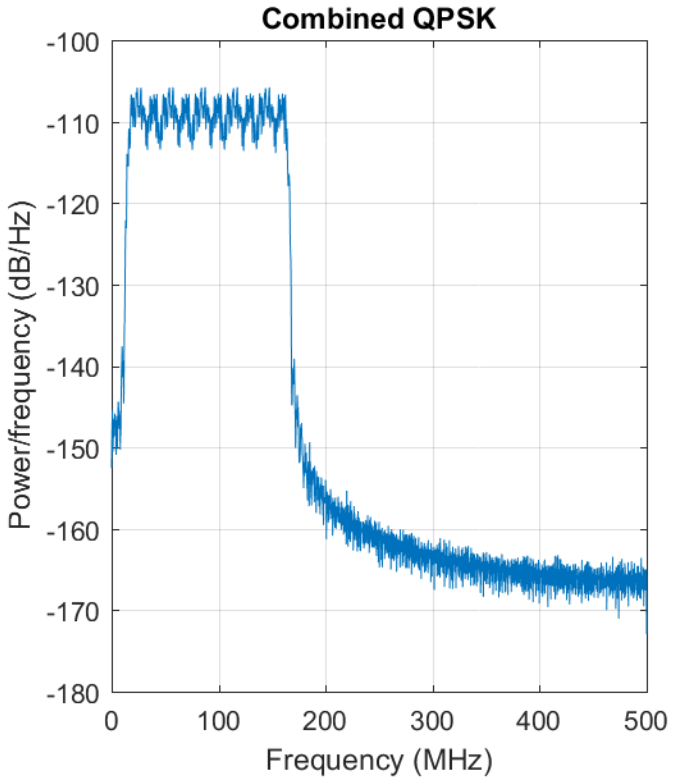

MME Detection Results

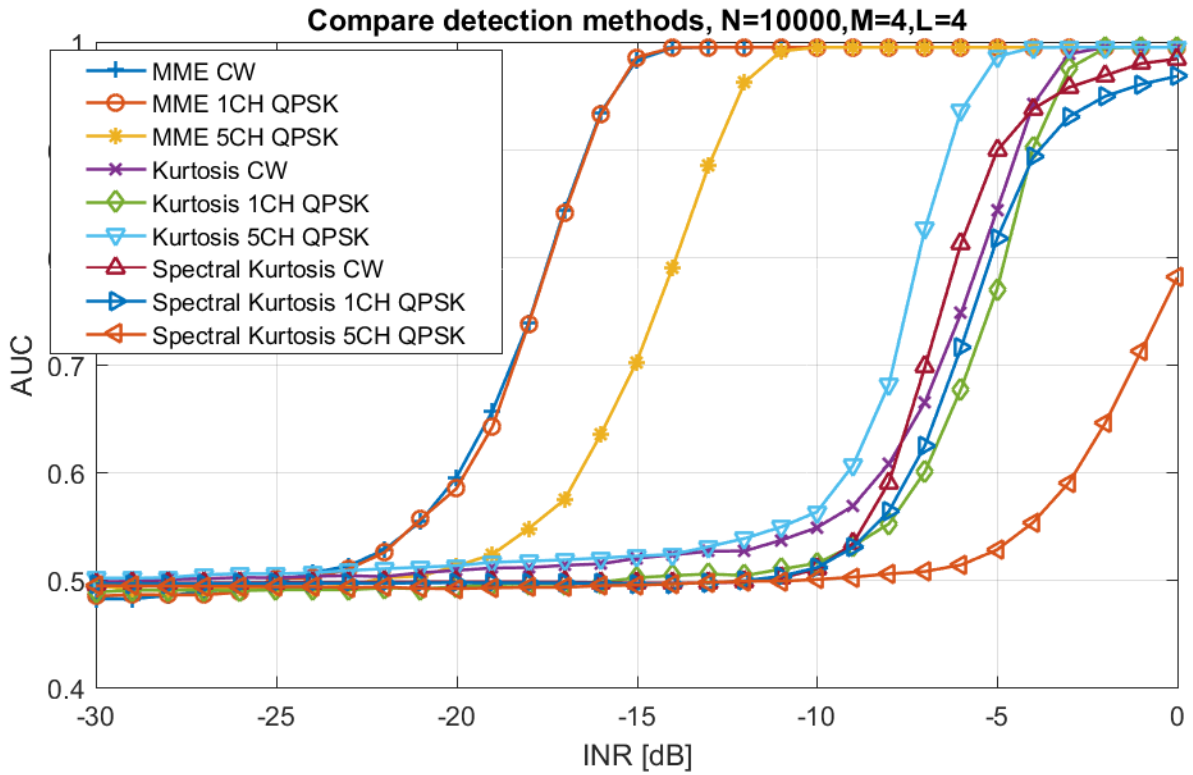

Eigenvalue Detection method greatly outperforms all other methods tested (Kurtosis[2,3] and Spectral Kurtosis[20])

RFI Excision Performance

Sample Variance
Compared to
Eigenvalue Variance Estimate

Eigenvalue Variance Estimate outperforms sample variance at interference levels of -14db INR and greater.

Eigenvalue variance estimate accuracy depends on the complexity of the RFI

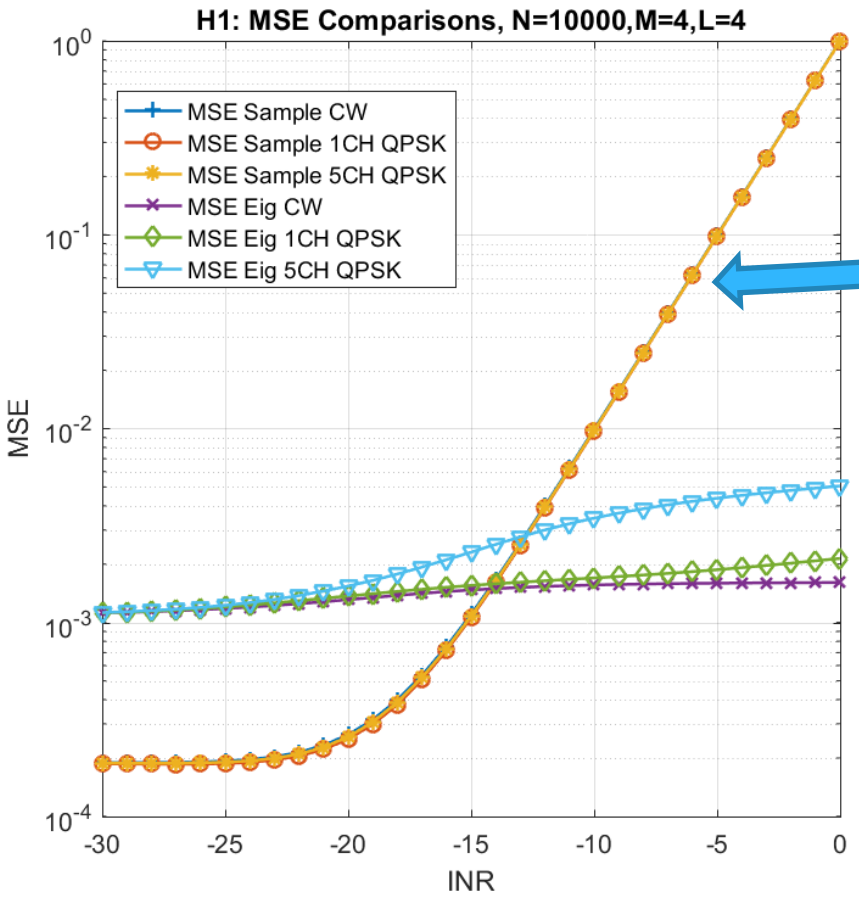

Sample Variance

Eigenvalue Estimate

References

1) Draper, David W., “Report on GMI Special Study #15: Radio Frequency Interference” , Ball Aerospace and Technologies Corp., Jan 16, 2015

2) De Roo, R.D.; Misra, S.; Ruf, C.S., "Sensitivity of the Kurtosis Statistic as a Detector of Pulsed Sinusoidal RFI," in Geoscience and Remote Sensing, IEEE Transactions on , vol.45, no.7, pp.1938-1946, July 2007

3) J. Piepmeier, J. Johnson, P. Mohammed, D. Bradley, C. Ruf, M. Aksoy, R. Garcia, D. Hudson, L. Miles,and M. Wong, “Radio-frequency interference mitigation for the soil moisture active passive microwave radiometer,” IEEE Transactions on Geoscience and Remote Sensing, vol. 52, no. 1, pp. 761–775, January 2014.

4) Bradley, D.; Morris, J.M.; Adali, T.; Johnson, J.T.; Aksoy, M., "On the detection of RFI using the complex signal kurtosis in microwave radiometry," in Microwave Radiometry and Remote Sensing of the Environment (MicroRad), 2014 13th Specialist Meeting on , vol., no., pp.33-38, 24-27 March 2014

5) A. J. Schoenwald, D. C. Bradley, P. N. Mohammed, J. R. Piepmeier and M. Wong, "Performance analysis of a hardware implemented complex signal kurtosis radio-frequency interference detector," 2016 14th Specialist Meeting on Microwave Radiometry and Remote Sensing of the Environment (MicroRad), Espoo, 2016, pp. 71-75.

6) A. Hyvärinen and E. Oja. Independent component analysis: algorithms and applications. Neural Networks 13, 4-5 (May 2000), 411-430

7) A. J. Schoenwald, A. Gholian, D. C. Bradley, M. Wong, P. N. Mohammed and J. R. Piepmeier, "RFI detection and mitigation using independent component analysis as a pre-processor," 2016 Radio Frequency Interference (RFI), Socorro, NM, 2016, pp. 100-104.

8) S. Misra, P. N. Mohammed, B. Guner, C. S. Ruf, J. R. Piepmeier and J. T. Johnson, "Microwave Radiometer Radio-Frequency Interference Detection Algorithms: A Comparative Study," in IEEE Transactions on Geoscience and Remote Sensing, vol. 47, no. 11, pp. 3742-3754, Nov. 2009.

9) A. Hyvärinen. “Fast and Robust Fixed-Point Algorithms for Independent Component Analysis”, IEEE Transactions on Neural Networks 10(3):626-634, 1999.

10) V. Zarzoso and P. Comon, "Robust Independent Component Analysis by Iterative Maximization of the Kurtosis Contrast with Algebraic Optimal Step Size", IEEE Transactions on Neural Networks, Vol. 21, No. 2, February 2010, pp. 248-261.

11) Mike Novey and T. Adali, "On Extending the complex FastICA algorithm to noncircular sources" IEEE Trans. Signal Processing, vol. 56, no. 5, pp. 2148-2154, May 2008.

12) X.-L. Li, and T. Adali, "Blind spatiotemporal separation of second and/or higher-order correlated sources by entropy rate minimization," in Proc. IEEE Int. Conf. Acoust., Speech, Signal Processing (ICASSP), Dallas, TX, March 2010.

13) Mike Novey and T. Adali, "Complex Fixed-Point ICA Algorithm for Separation of QAM Sources using Gaussian Mixture Model" in IEEE Conf. ICASSP 2007

14) G.-S. Fu, R. Phlypo, M. Anderson, and T. Adali, "Complex Independent Component Analysis Using Three Types of Diversity: Non-Gaussianity, Nonwhiteness, and Noncircularity," IEEE Trans. Signal Processing, vol. 63, no. 3, pp. 794-805, Feb. 2015.

15) ICA and BSS Group, Aalto University, Matlab Resources, http://research.ics.aalto.fi/ica/fastica/

16) Vicente Zarzoso, Institut Universitaire de France , Robust ICA, Matlab Resources, http://www.i3s.unice.fr/~zarzoso/robustica.html

17) Machine Learning for Signal Processing Laboratory, University of Maryland Baltimore County , Matlab Resources, http://mlsp.umbc.edu/resources.html

18) Y. Zeng and Y. C. Liang, "Eigenvalue-based spectrum sensing algorithms for cognitive radio," in IEEE Transactions on Communications, vol. 57, no. 6, pp. 1784-1793, June 2009.

19) Bai, Z. D. Methodologies in Spectral Analysis of Large Dimensional Random Matrices, A Review Statistica Sinica, 1999 , 9 , 611-662

20) Nita, G. M.; Gary, D. E.; Liu, Z.; Hurford, G. J. & White, S. M. Radio Frequency Interference Excision Using Spectral-Domain Statistics Publications of the Astronomical Society of the Pacific, 2007 , 119 , 805-827